Surface of Poly(ethylene terephthalate/isophthalate) Copolyesters Studied by Atomic Force Microscopy

D. A. SCHIRALDI,[1]* S. A. C. GOULD,[2] AND M. L. OCCELLI[3]

[1] KoSa, P. O. Box 5750, Spartanburg, South Carolina 29304

[2] W. M. Keck Science Center, Claremont College, Claremont, California 91711

[3] MLO Consulting, 6105 Blackwater Trail, Atlanta, Georgia 30328

Received November 9 1999; accepted June 3 2000

ABSTRACT: An atomic force microscope (AFM) operating in Tapping™ and contact modes has been used to study the surface topography and the molecular organization of poly(ethylene terephthalate) (PET) films containing 2% (PET-2I) and 10% (PET-10I) isophthalate, and of injection/blow molded bottles containing 2.6% (PET-2.6I) and 10% isophthalate. Large-scale (15-μm $\times$ 15-μm) AFM images have shown that both surfaces are fairly flat and heterogeneous in nature, often containing inclusions. Whereas the PET surface appears to be formed mainly by microfibrils, isophthalic acid (IPA) incorporation at the 2–10 mol % level gives the surface a granular appearance. The IPA-containing PET surfaces are frequently coated by a lacelike film consisting of submicron "beads" joined together by filaments. These "strings of beads" form bundles and can also connect bundles. AFM images of PET-2I closely resemble those generated for PET films. By contrast, the lacelike structure becomes a dominant feature of the PET-10I surface. The level of inclusions observed on film surfaces appears to correlate with the levels of extractable oligomers present in the polymers. Nanometer-scale AFM images of PET-10I exhibit surfaces composed of short stacks of plates or rods, with 30–50-nm voids or pores between these stacks. Whereas surface deposits of what we suggest is most likely an oligomer correlates with isophthalate concentration, we see no gross structural features in PET-2I and PET-10I that explain the observed improvement in gas diffusion barrier in these polymers. © 2001 John Wiley & Sons, Inc. J Appl Polym Sci 80: 750–762, 2001

Key words: PET; AFM; Tapping™ and contact modes; gas diffusion barrier; oligomer

INTRODUCTION

Over the past 30 years, poly(ethylene terephthalate) (PET) has grown to be the dominant packaging material for a variety of applications that include carbonated beverages, bottled waters, and isotonic sports drinks. The wide acceptance of PET is a result of a combination of its favorable mechanical and barrier properties, low cost, and ready recyclability. Whereas PET packages in North America are generally given the PET-1 recycling label, the polymers used in such applications are, in fact, minor copolymers of PET. Typical co-monomers incorporated into the chemical backbone of PET for packaging applications include 1,4-cyclohexanedimethanol, diethylene glycol, and especially isophthalic acid, IPA. Incorporation of IPA into PET reduces the rate of crys-

Correspondence to: D. A. Schiraldi.

Journal of Applied Polymer Science, Vol. 80, 750–762 (2001)

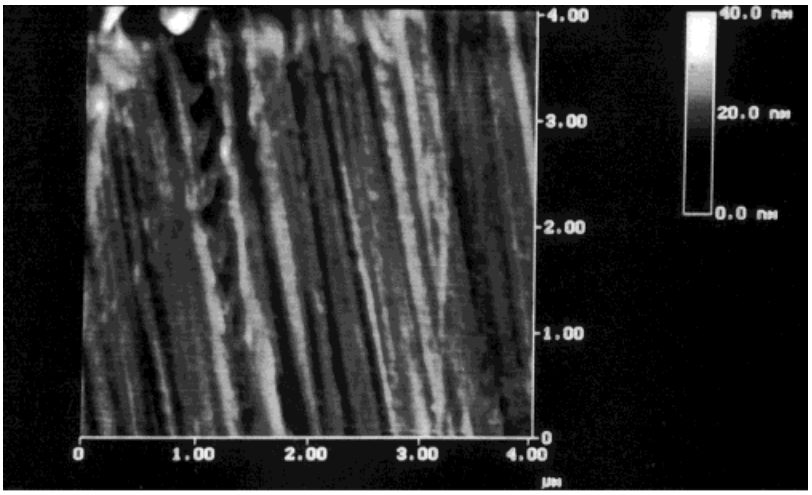

(A)

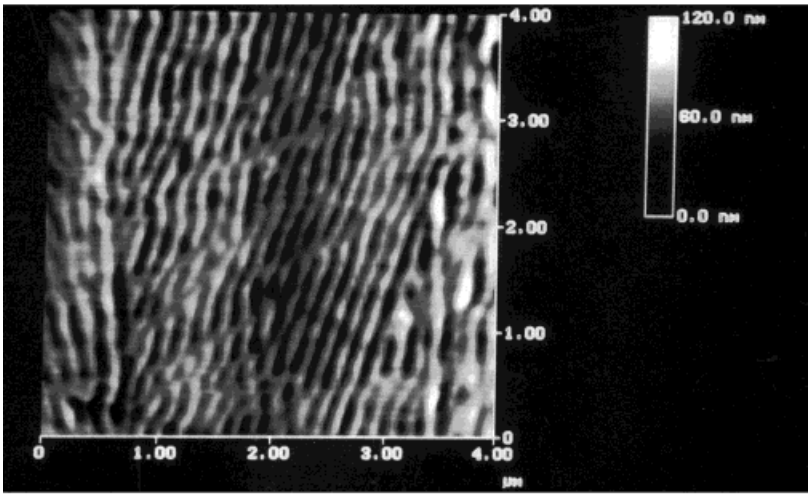

(B)

Figure 1 Micrometer-scale contact-mode atomic force microscopy (AFM) images in air of the reference poly(ethylene terephthalate) (PET) film. Top view images of (A) a densely packed ordered array of fibrils (crystalline zone); (B) a densely packed but highly disordered array of fibrils (an amorphous zone); (C) both amorphous and crystalline zones; and (D) the PET surface crossed by fibrils consisting of "string of beads."

tallization of semicrystalline PET, generally without reducing its ultimate attainable level of crystallinity or mechanical or gas barrier properties. In fact, recent work by manufacturers such as BP-Amoco (supplier of IPA) and KoSa (supplier of PET) has demonstrated that carbon dioxide and oxygen barrier properties are actually enhanced by increasing IPA levels in PET/IPA copolymers. Incorporation of approximately 10 mol % of isophthalate appears to give an optimum improvement in gas barrier (approximately 20% improvement for carbon dioxide and oxygen)[1] while maintaining the mechanical and processability properties of the PET polymer. It is not intuitively obvious that incorporation of a monomer, designed to inhibit crystallization, would improve the barrier properties of a polymer gas.

The purpose of this work is to describe the surface topography of PET-I surfaces, using an atomic force microscope operating in (1) Tapping™, to give micrometer-scale details; and (2) contact mode, to provide molecular-scale resolution of the surface. Tapping™ mode is a registered trademark of Digital Instruments (Santa

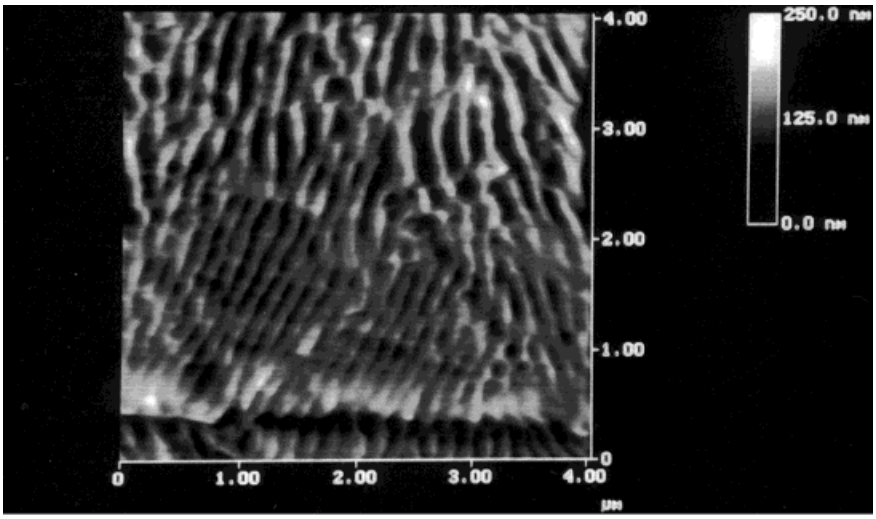

(C)

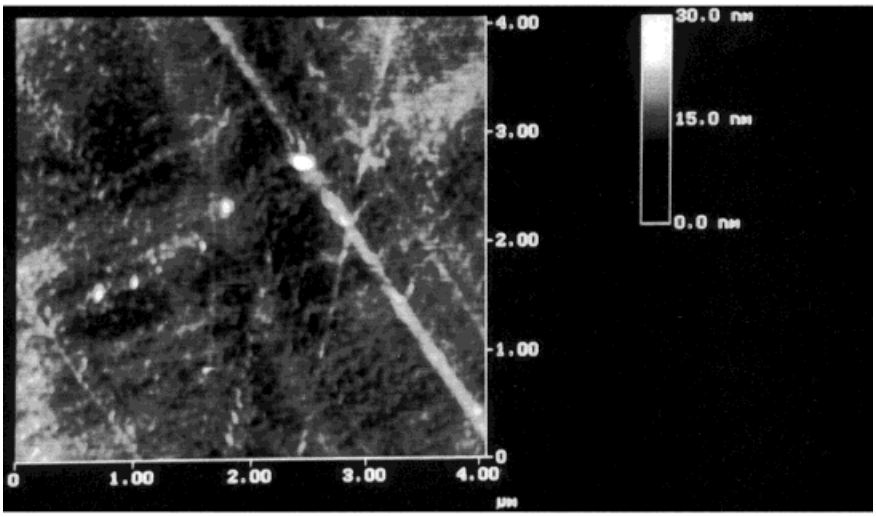

(D)

Figure 1 (*Continued from the previous page*)

Barbara, CA). Further, an objective of this work is to observe possible changes in polymer surface architecture that result upon incorporation of 2–10 mol % isophthalate into PET. It is hoped these results will lead to greater understanding of the isophthalate effect in PET copolymer barrier resins.

EXPERIMENTAL

The PET and PET-I polymers used in this study were produced from dimethyl terephthalate (DMT), dimethyl isophthalate (DMI), manganese acetate, antimony oxide, and polyphosphoric acid in a 3000-lb batch autoclave system, operating under normal commercial PET conditions.[2,3] The resultant 0.62-intrinsic viscosity (IV) polymers were solid-state polymerized at 210°C/vacuum to yield a 0.84-IV copolyester resin.

Intrinsic viscosity measurements reported are for 4% w/w solutions in *o*-chlorophenol at 25°C. Isophthalate levels reported are calculated by the following equation:

$$100\% \times (\text{mol \% isophthalate}) / [(\text{mol \% isophthalate}) + (\text{mol \% terephthalate})]$$

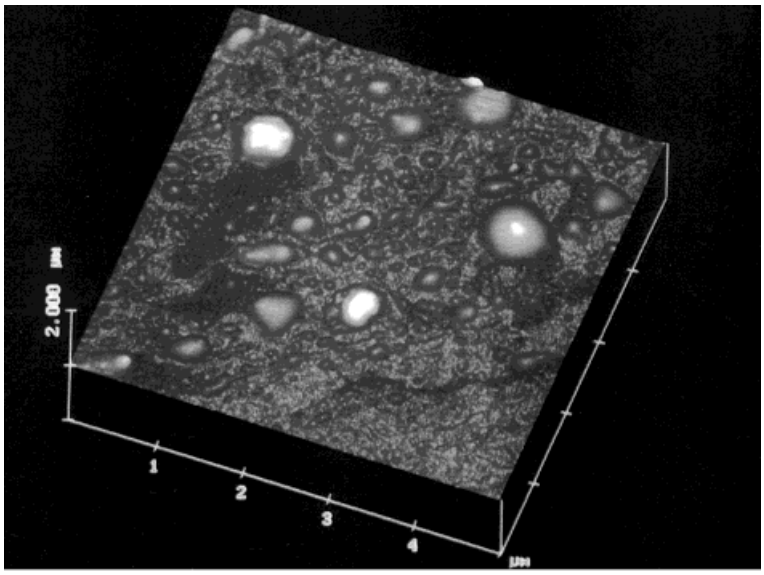
2.000 µm
1
2
3
4
µm

(A)

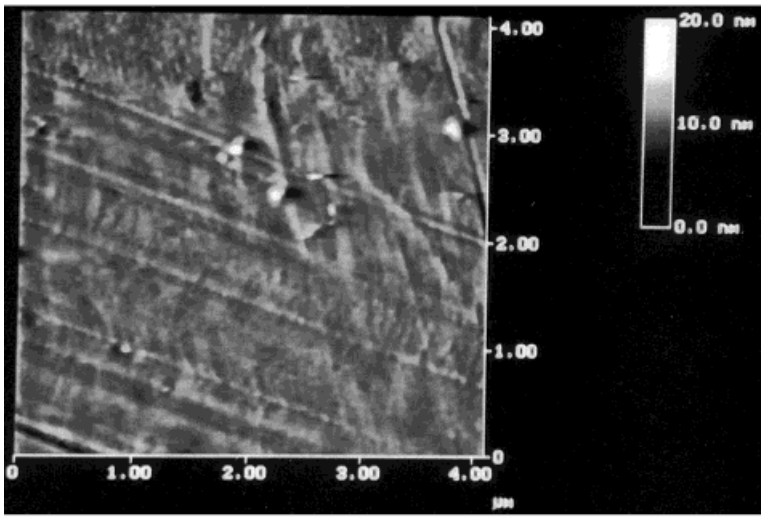
4.00
3.00
2.00
1.00
0
0
1.00
2.00
3.00
4.00
µm
20.0 nm
10.0 nm
0.0 nm

(B)

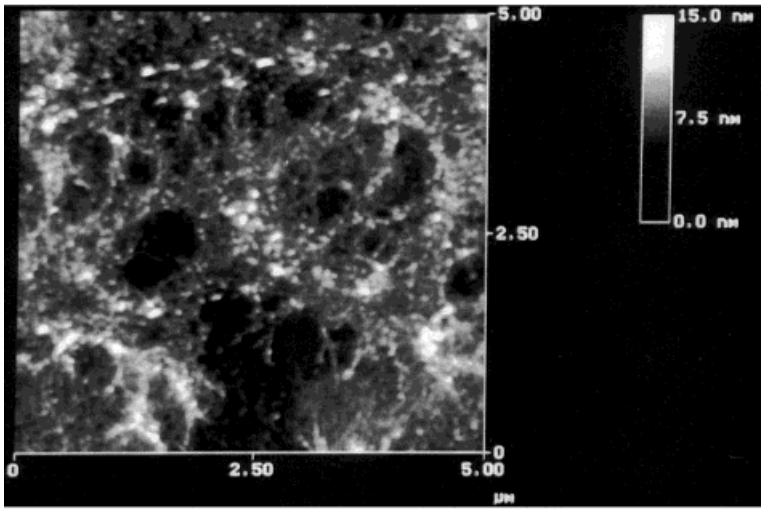
5.00
2.50
0
0
2.50
5.00
µm
15.0 nm
7.5 nm
0.0 nm

(C)

Figure 2

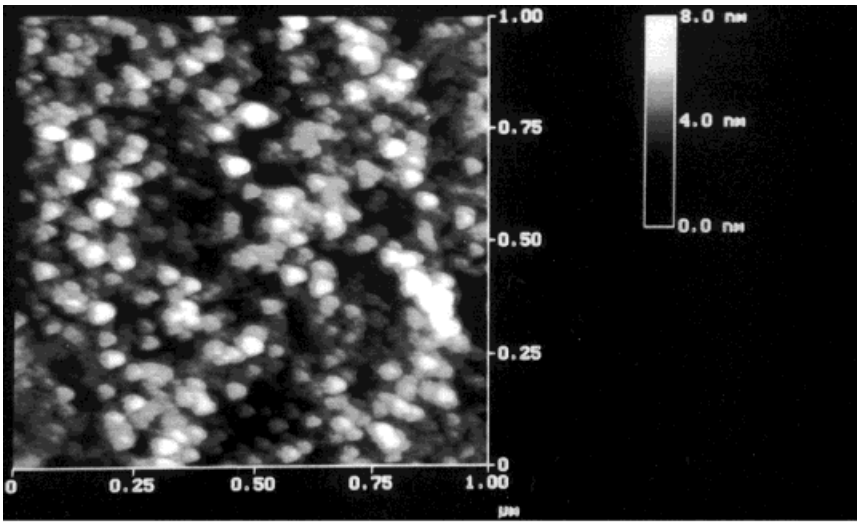

(D)

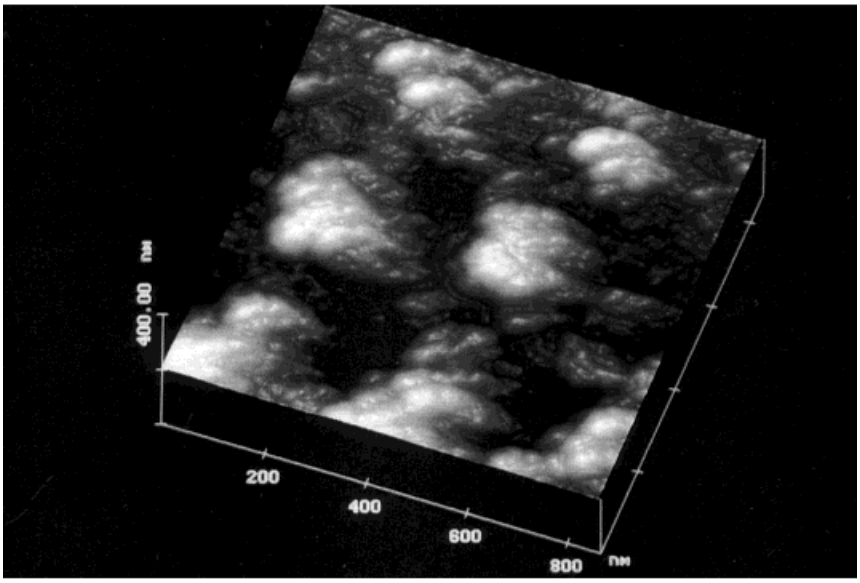

(E)

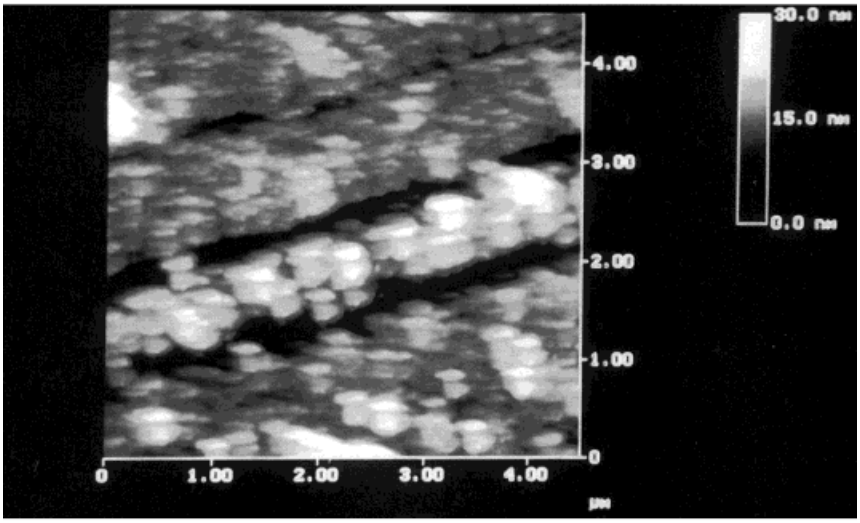

(F)

Figure 2 (*Continued from the previous page*)

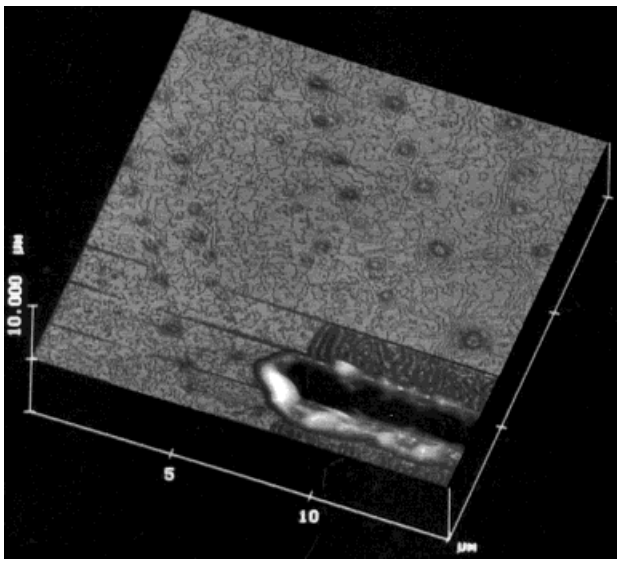

Figure 3 Contact-mode atomic force microscopy (AFM) images in air of the PET-2I film showing surface deformation induced by the imaging force.

Incorporated isophthalate compositions were confirmed by 300-MHz proton NMR; retained compositions closely followed charged compositions.

The 0.84-IV copolyester resins (0%, 2%, 10% isophthalate) were melt-extruded at 285°C through a standard film die to yield the undrawn, air-quenched 0.3-mm film samples used in this study.

Samples of 0.84-IV copolyester resins (2.6%, 10% isophthalate) were injection molded into 11.7:1 NSR tooling bottle preforms (average melt temperature 285°C), then blow molded (average temperature 100°C) into 0.5-L carbonated soft drink bottles.

Oligomer levels in PET and PET-I10 were determined by grinding, sieving, and weighing samples of the polymers, soxhlet extracting overnight with $CDCl_3$, followed by quantification using 300-MHz proton NMR spectroscopy.

Film and razor-cut bottle sidewall samples were glued onto steel disks with epoxy. After the glue dried, the AFM tip was carefully guided to the middle of the film, thus beginning the imaging session. The AFM used in this work was a Nanoscope III instrument (from Digital Instruments, Santa Barbara, CA) operating in contact mode or Tapping mode. As in previous work,[4,5] the AFM was calibrated using mica. The images presented in this paper contain either 256 × 256 or 512 × 512 data points and were obtained within a few seconds. The Si_3N_4 cantilevers used (with integral tip) had a length within the 60–120-μm range with a spring constant of 0.1–0.6 N/m. The typical force applied to obtain these images ranged within 1.0–100 nN. Several hundred images were examined, using different cantilevers. In order to avoid tip-related artifacts,[5] imaging was performed with minimal (<10 nN) force and image features were reproduced in both Tapping and contact mode before being accepted as representative.

RESULTS AND DISCUSSION

In recent years, scanning probe microscopy such as AFM has become an imaging technique of particular utility for the study of a variety of surfaces at the molecular-scale level.[6–8] In two companion articles,[4,5] contact-mode AFM images were used to describe PET films and liquid crystalline polymer (LCP) surfaces with molecular-scale resolution. Resolution is in general controlled by the size of the contact area between the tip and the polymer surface. It is for this reason then, in studies of polymer surfaces, that low force and force depending imaging is performed.[9,10] Tip-induced surface deformations were nonetheless observed to occur when imaging PET type films.[4] In the present article, an AFM operating in Tapping mode has been used to reduce the contact force and contact time between tip and sample as a means of minimizing tip-induced damage and artifacts.

Poly(ethylene Terephthalate) Films

Contact-mode AFM images of PET film surfaces are presented in Figure 1. These images show

Figure 2 (*Continued from the previous page*) Micrometer-scale Tapping-mode™ atomic force microscopy (AFM) images in air of the poly(ethylene terephthalate) (PET) film after 2% isophthalic acid showing (A) surface debris; (B) raised surface features crossing the film surface; (C) the appearance of lacelike structure on the film surface; (D) the appearance of granules on the PET-2I surface, (E) granules agglomeration and surface porosity, and (F) details of a thermally treated PET-2I film.

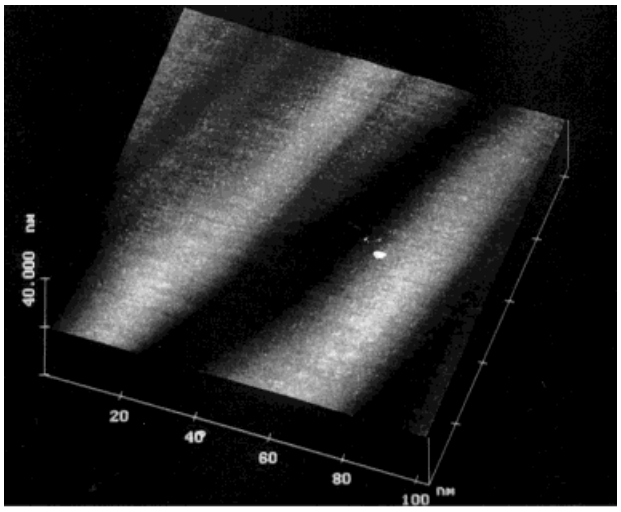

(A)

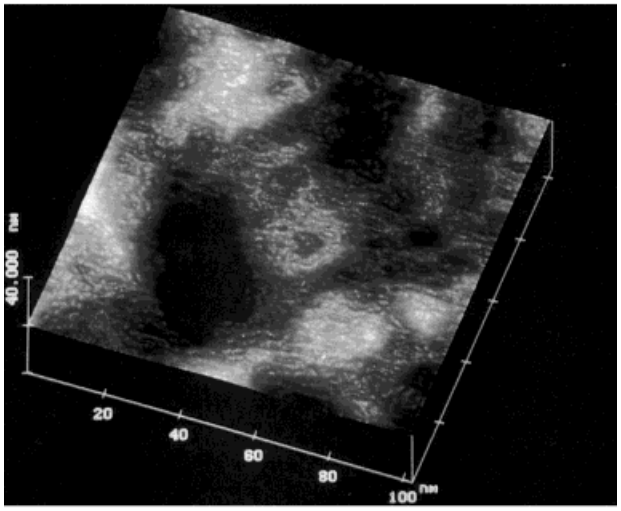

(B)

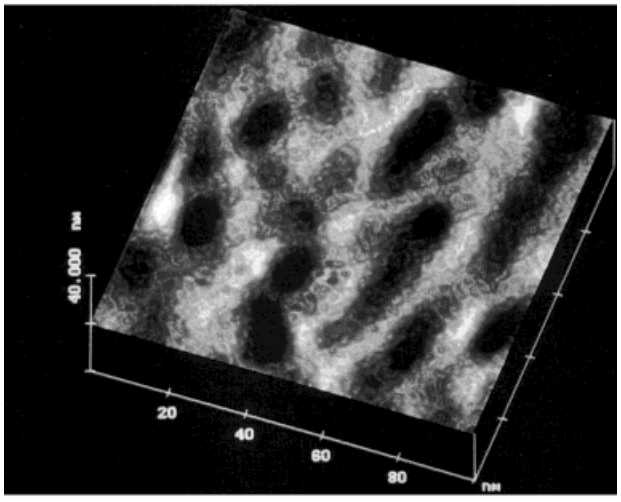

(C)

raised ridges, 80–200 nm in width and 2–10 nm in height, aligned along what is believed to be the PET film extrusion direction (Fig. 1A). Variations in structure were found within the same sample (Fig. 1B–D). In some regions, ridges were found to split and change orientation, to terminate into other ridges, and to merge together as shown in the densely packed but not highly ordered array of fibrils in Figure 1A. Other regions of the same samples show little texture (Fig. 1D). The difference in surface roughness between areas containing large ridges and those with fewer features is approximately a factor of 10; it is unclear whether these differences reflect crystalline vs. amorphous regions of the polymers, or different crystalline morphologies that may result during air quenching of the film samples from the melt. Generally apparent is directionality in the samples, which we attribute to the "machine direction" of the extruded films. Whereas the samples were not intentionally drawn, an inherent orientation process always occurs during melt extrusion. Whereas the parallel ridges observed in Figure 1A could reasonably be attributed to die marks, one would expect consistent marks across the film samples (not observed). The more complex fibular structure of Figure 1B,C is also inconsistent with die marks, as are the nonparallel linear structures of Figure 1D. Also noteworthy is that the flat PET surfaces can be dotted with small "beads" and that these beads can agglomerate to form randomly oriented ridges with widths of 50–160 nm.

PET/2% Isophthalate Copolyesters (PET-2I) Films

The effects of 2% isophthalate incorporation into PET on the polymer topography are shown in Figure 2. Images were taken operating the AFM in a Tapping™ mode, since the imaging force in contact mode can alter the soft surface of the film irreversibly, as indicated in Figure 3. Large-scale AFM images represent the PET-2I surface as flat and relatively featureless, dotted with surface particles (Fig. 2A) The largest surface particle in this figure is about 800 nm in size and is 50 nm

Figure 4 Nanometer-scale tapping mode atomic force microscopy (AFM) images in air of the PET-2I film showing (A) the presence of fibrils; (B) the existence of large mesopores; and (C) pore size distribution and related surface morphology.

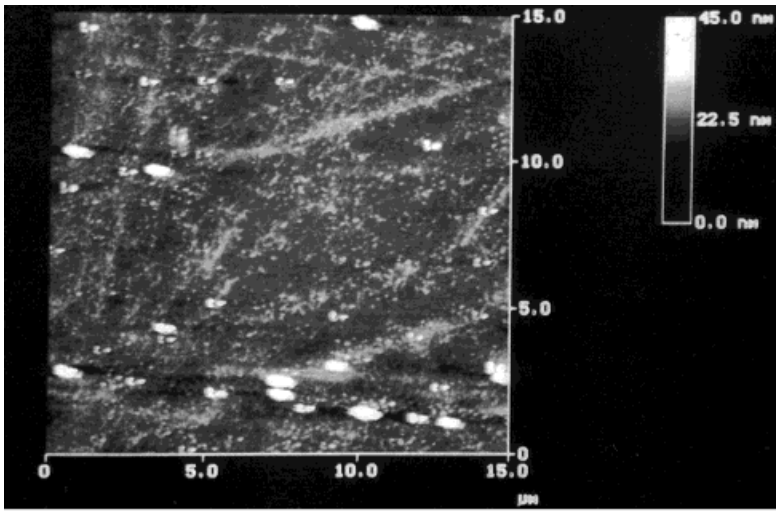

(A)

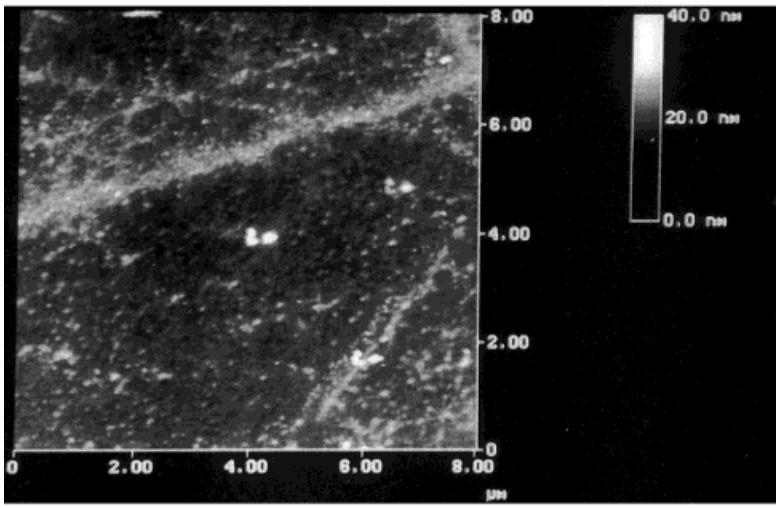

(B)

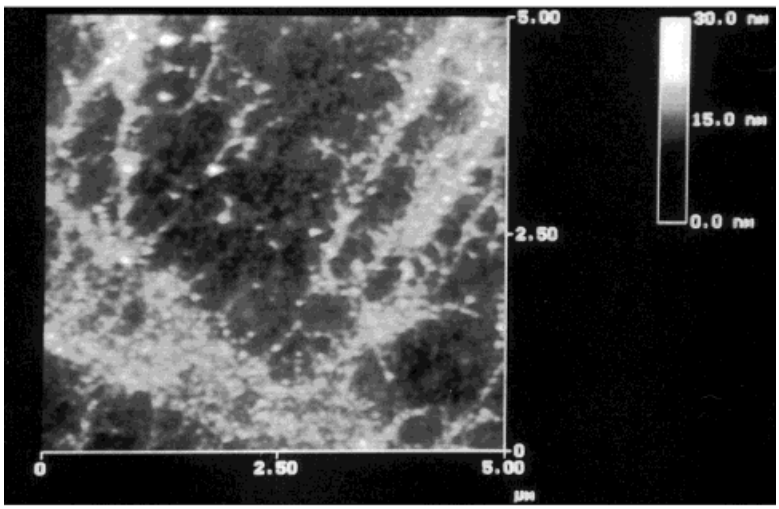

(C)

Figure 5 Micrometer-scale tapping-mode mode atomic force microscopy (AFM) images in air of the PET-10I film showing (A) a typical lacelike structure on the film surface; (B) an example of a "string of beads" in which the small granules that form this raised surface ribbon, are clearly visible; and (C) the large width of the ribbons, with a the lacelike structure, that crisscross the film surface.

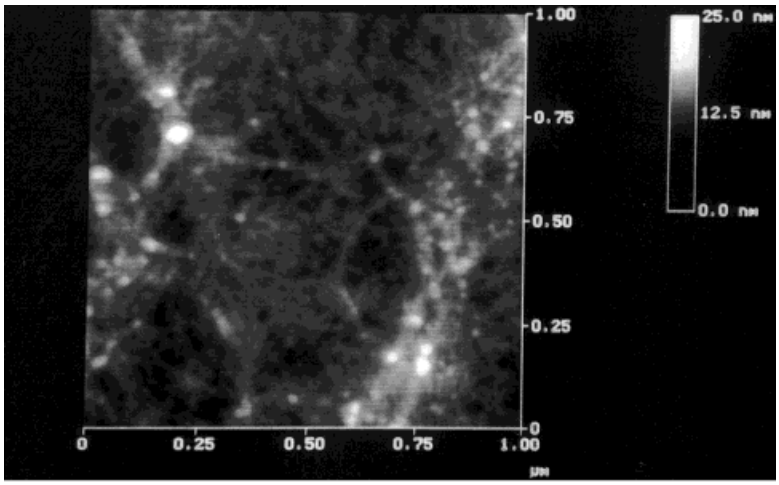

(A)

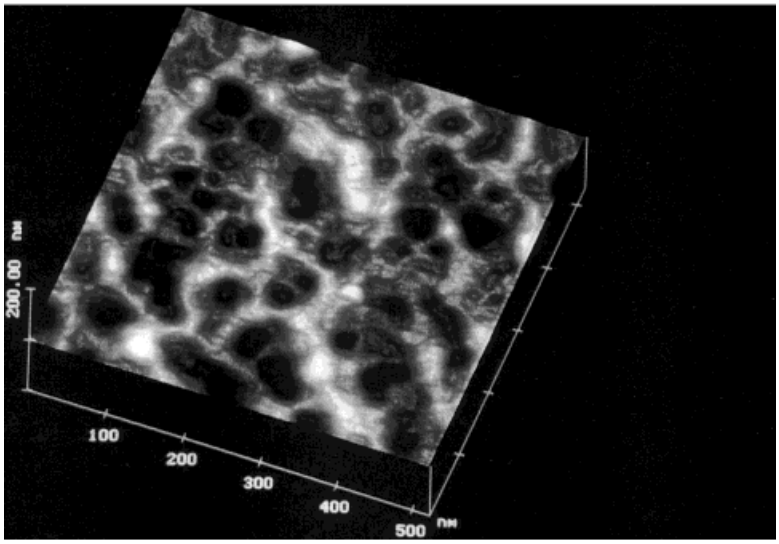

(B)

Figure 6 Tapping-mode™ atomic force microscopy (AFM) images in air showing of the PET-10I showing (A) details of the lacelike structure that cover the film; (B) pore size distribution and surface morphology; (C) the existence of large mesopores on the film surface; and (D) the existence of densely packed short fibrils and voids on the film surface.

thick. As observed in the parent PET film, the surface can contain ribbon-shaped fibrils (Fig. 2B); these fibril are not present consistently in the sample, leading us to reject the possibility that these are die marks. Finally, the PET-2I surface appears to be granular in some regions and in other locations to have a lacelike structure resembling a crust on top of the polymer matrix (Fig. 2C). The image in Figure 2C represents one of the few images obtained showing the surface supporting a lacelike structure not observed in any images of the reference PET surface.

At higher magnification, the PET-2I surface appears granular. Cross-sectional analysis of the surface[12] in Figure 2D computes the diameter of the granules to be within the 40–600-nm range. Frequently these particles form agglomerates; in Figure 2E the largest agglomerate is 250 nm wide and about 10 nm tall. Interestingly, the stacking of short rods or plates appears as the main feature in the image of a PET-2I film that has been melted, see Figure 2F. Missing plates (or rods) initiate long cracks on the surface about 250 nm in width, Figure 2F.

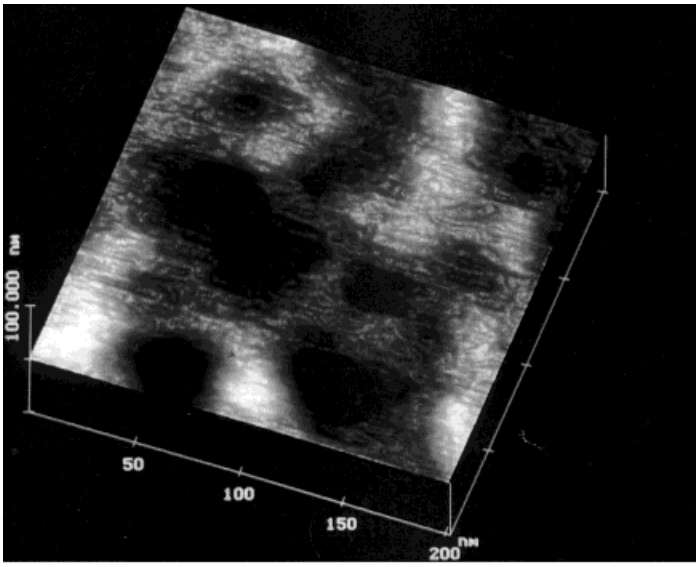

(C)

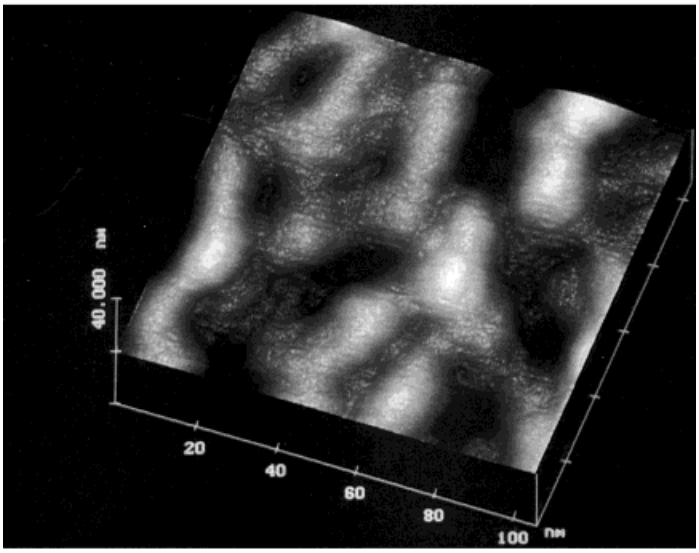

(D)

Figure 6 (*Continued from the previous page*)

Nanometer-scale images in Figure 4A–C indicate a lack of ordered structural details and of recognizable structural features. The surface can be corrugated, as in Figure 4A, or it may contain pits about 200 nm deep and 150 nm wide, as in Figure 4B. Evidence of surface pores can be seen in the 100-nm × 100-nm image in Figures 4C. Distribution of pits and valleys on the surface is not homogeneous and a compact surface with a distribution characterized by shallow pits, 5–10 nm wide and 0.1–0.2 nm deep, of the type shown in Figure 4C is a common occurrence.

PET/10% Isophthalate Copolyesters (PET-10I) Films

After increasing the isophthalate level in PET from 2% to 10%, the PET surface topography change as indicated in Figures 4–6. The large (15-μm × 15-μm) scale AFM image in Figure 5A, for PET-10I, reveals a fairly flat surface crisscrossed by randomly oriented filaments. These filaments can coalesce and form ribbons of variable width, as shown in Figure 5B,C. This lacelike structure is dotted with inclusions that are irregular in size and shape. In Figure 5C, surface

Table I Correlation Between Bulk Isophthalate Concentration and Extractable Oligomer Levels in PET/Isophthalate Copolymers

Mol % Isophthalate in PET-I	Wt % Extracted Oligomers
0	1.2
2	1.4
10	2.5

PET, poly(ethylene terephthalate).

"beads" have a diameter within the 50–100-nm range and form a ribbon with a lacelike appearance 1.2 μm wide.

Details of the surface filaments are shown in the 1 μm $\times$ 1 μm Tapping mode AFM image in Figure 6A. The lace structure that cover the PET-10I surface appears to be formed by nanometer-scale "beads" joined together by a microfibril 20–25 nm in width. "Strings of beads," 20–50 nm in diameter, form bundles and can extend and connect bundle to bundle. The possibility that during the film forming process, specific polyester oligomers are bloom to the surface forming the details shown in Figure 5A–C, was considered a distinct possibility, so the relative amounts of extractable oligomers in the PET homopolymer and PET-I10 copolymer were tested (Table I). Extraction of the samples yielded oligomer levels roughly proportional to the isophthalate concentration (Table I).

Thus, the oligomer analysis is wholly consistent with the increasing level of particulate inclusions on film surfaces, as isophthalate content is increased in the polymer. ^{1}H-NMR results have indicated that the extracted oligomers are a mixture of ethylene isophthalate cyclic dimer, various ethylene isophthalate/terephthalate trimers, and higher oligomers; a significant effort at characterizing these materials in detail was not made. It should be pointed out that the increase in oligomer content observed by soxhlet extraction of the polyesters is not observed by high-performance liquid chromatography (HPLC) analysis until isophthalate levels are increased to $>$40 mol %.[13]

It is often possible to observe regions of the PET-10I surface that are free from filaments. Tapping-mode AFM image images show that these regions are fairly inhomogeneous and contain several craterlike depressions 40–50 nm in diameter and 1–2 nm deep (Fig. 6B). At higher magnification, short rods can be observed to separate the various surface depressions; missing plates form voids or surface opening 30–50 nm in diameter and about 1–2 nm deep (Fig. 6C). The geometry and size of these pores depend on the mode of aggregation of the different particles that form the surface (Fig. 6D). Cross-sectional analysis of the image shows that the average rod length is 40 nm and that the width is within the 12–16-nm range.

If the hypothesis of copolyester surfaces contaminated by particles and networks of oligomeric material is correct, the images presented in this study represent the inherent polymer structures and its surface contaminants. Knowing that, in condensation polymers (e.g., the PET-I copolymers of this study), oligomers are always in thermodynamic equilibrium with higher polymers, and that blooming of small molecules contained in polymer matrixes is a normal phenomenon in plastics processing, we consider the detailed characterization of such complex surfaces to be of value.

PET/2.6% (PET-2.6I) and PET/10% Isophthalate (PET-10I) Copolyester Bottles

AFM Images of injection-blow molded bottles of PET-2.6I (Fig. 7A–C) and of PET-10I (Fig. 7D–F) are shown below. In these images, both similarities and differences between bottle and film samples are apparent. Fibular structures are observed in the bottle samples, but to a much lower extent than in films (e.g., cf. Fig. 7B and E vs. Figs. 2B and 6A). We attribute this result to the difference between uniaxial orientation (that is unavoidable during melt extrusion of film) and the radial biaxial orientation (which is inherent in bottle blowing). Surface debris is apparent in all the blow-molded surfaces, and again debris becomes more prevalent with higher isophthalate levels in the constituent polymers (cf. Fig. 7A and D vs. 7C and D). If the hypothesis is correct that this debris is oligomeric material, one can reasonably expect debris to be present in all manner of samples; the size/shape of the oligomer deposits would in part reflect the thermal history of the plastic objects subjected to blooming of small molecules. Figure 7C shows a molded feature that possesses a smooth rather than a gauged texture that appears to be part of the bottle design.

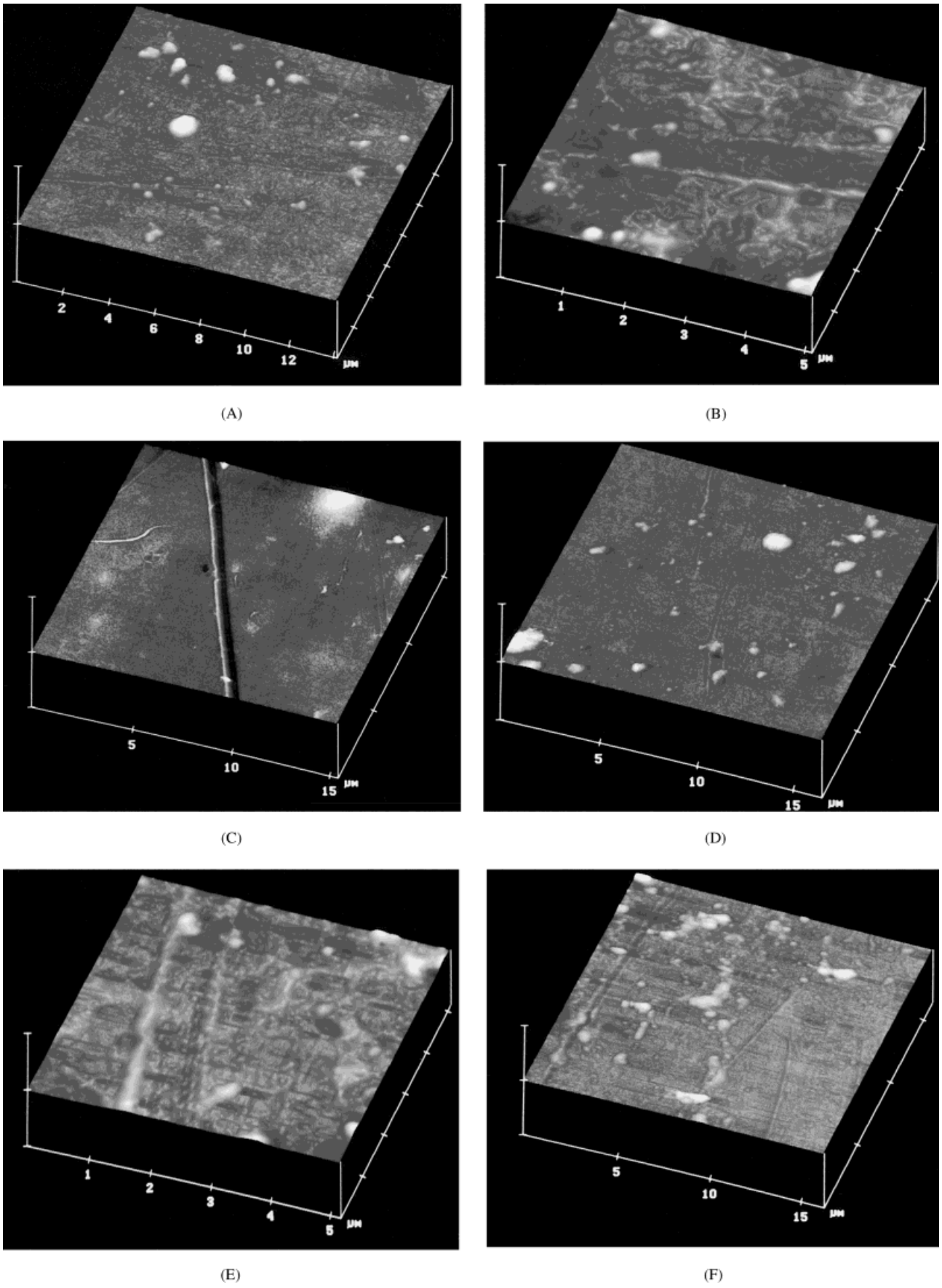

Figure 7 Tapping-mode™ atomic force microscopy (AFM) images of PET-2.6I (A–C) and PET-10I (D–F) injection/blown bottle surfaces.

SUMMARY AND CONCLUSIONS

AFM images show the PET surface consisting of fibrils irregular in size and shape. These fibrils can align along a preferential direction forming crystalline domains, or can have variable direction, size, and shape generating amorphous regions that increase the surface roughness.

After the addition of 2 mol % isophthalic acid, many of the features of the parent PET surface are retained. However, in addition to fibrils, the surface contains regions consisting of granules as well as regions in which a lacelike structure is overlaid on the film surface. This type of surface detail was not observed in any AFM images of the parent PET sample.

When the isophthalic acid level is increased from 2% to 10%, the appearance of the aforementioned lacelike structure becomes an easily observable surface feature. The structure consists of submicron particles or granules connected by a fine filament or microfibril. Microfibrils can agglomerate forming bundles that cross the surface in a random direction. The nature of the lacelike structure observed to increase with IPA levels remains poorly understood, but the increasing level of inclusions observed as isophthalate content is increased correlates well with the level of extractable oligomers present in the polyesters. We tentatively conclude that the surface particles and lacelike structures are PET-I oligomers, which are always in thermodynamic equilibrium with high-molecular-weight polyesters, and are subject to blooming to plastic surfaces during processing.

Bottle sidewall samples exhibit little of the uniaxial structure observed on the surfaces of extruded films. We believe that this difference results from the radial biaxial orientation of blown bottles, versus the linear uniaxial drawing that occurs unavoidably during film production.

Whereas surface deposits of what we suggest is most likely oligomer correlates with isophthalate concentration, we did not observe any gross structural features in PET-2I and PET-10I films that explain the observed improvement in gas diffusion barrier, which tracks with increased isophthalate content in the polymer.

The support and many useful discussions with Dr. E. Paschke (BP-Amoco) are gratefully acknowledged. Special thanks are due to Mr. J. Kelly (BP-Amoco) for sample generation, to Dr. J. Pickett (UNCC Regional Analytical Facility) for oligomer testing, and to Susan Occelli for preparing this manuscript.

REFERENCES

1. van Haelst, L.; Bauer, C. W. Polyester ’97; Zurich, Nov. 3–5, 1997.
2. Whinfield, J. R.; Dickson, J. T. Brit Pat 578,079 (1946).
3. Whinfield, J. R.; Dickson, J. T. US Pat 2,465,319 (1949).
4. Gould, S. A. C.; Schiraldi, D. A.; Occelli, M. L. J Appl Polym Sci 1997, 65, 1237.
5. Gould, S. A. C.; Schiraldi, D. A.; Occelli, M. L. J Appl Polym Sci 1999, 74, 2243.
6. Binnig, J.; Rohrer, H.; Gerber, C.; Weibel, E. Phys Rev Lett 1983, 50, 120.
7. Albrecht, T. R.; Dovek, M. M.; Lang, C. A.; Grutter, P.; Quate, C .F.; Kuan, S. N. J.; Frank, C. W.; Pease, R. F. W. J Appl Phys 1988, 64, 1178.
8. Nagy, K. L.; Blum, A. E., Eds. Scanning Probe Microscopy of Clay Minerals; CMS Workshop Lectures, Vol 7; The Clay Mineral Society, 1994.
9. De Neve, T.; Navard, P.; Kleman, M. J Rheol 1993, 37, 515.
10. Bengel, H.; Cantow, H.-J.; Magonov, S. N.; Monconduit, L.; Evain, M.; Whangbo, M.-H. Surf Sci Lett 1994, 321, L170.
11. Digital Instrument SPM Training Notebook; 1996; p 47.
12. Digital Instrument Command Reference Manual; 1997; p 12.
13. BP Amoco Corporation, unpublished results.